

**〈Technical Note〉**

**A Coherent Methodology for the Evaluation of a Steam  
Explosion Load Using TEXAS-V**

**Jin Ho Song, Ik Kyu Park, and Jong Hwan Kim**

Korea Atomic Energy Research Institute  
150, Deokjin-dong, Yuseong-gu, Daejeon, 305-353, Korea  
dosa@kaeri.re.kr

(Received April 23, 2004)

**Abstract**

A methodology is proposed for the evaluation of a steam explosion load on a reactor scale by evaluating the steam explosion model against the experimental data. Being part of the OECD/SERENA program, appropriate data was selected by international experts and the analytical model of TEXAS-V was chosen. The procedure consists of two steps. The pre-mixing model was verified against the FARO L-14 and FARO L-28 data. The explosion model was verified against the experimental data of KROTOS-44, FARO L-33, TROI-13, and TROI-34. The capabilities and deficiencies of the fundamental models of the TEXAS-V are reviewed in terms of their adequacy in a simulation of steam explosion on a reactor scale.

**Key Words** : steam explosion, TEXAS-V, FARO, KROTOS, TROI

**1. Introduction**

A computational model for the steam explosion phenomena [1] should be able to describe multi-phase, multi-dimensional, and multi-component phenomena at different length scales. The fundamental phenomena involved is melt jet break up and interfacial heat transfer between the melt and the two-phase mixture during the mixing phase, which occurs in an matter of seconds, and the thermal-hydrodynamic fragmentation and heat transfer during the explosion phase, which occurs in an matter of ms. The length scale involved in those processes has a wide range, from the scale of the jet diameter to the fine particles. So,

constructing even a simplified model is a formidable task.

Here, a rather simplified computational model to simulate the various phases of steam explosion phenomena is used to simulate the carefully selected international experimental data. The computational model is TEXAS-V, which is widely used for analysis of steam explosion load during simulations of severe accidents in nuclear power plants in which a molten core material at a very high temperature is in contact with water. Studying the computational model against the selected experimental data is part of an international collaboration called the OECD/SERENA research project. The objective of this

research is to pursue a collective understanding of the fundamental physics of steam explosion phenomena, which is necessary to predict the steam explosion load on a reactor scale and to identify the shortcomings of the existing models and experimental data [2].

Two sets of experimental data were carefully selected to validate the major physical models of the computational model in the OECD/SERENA program. The experimental data of FARO L-14 and L-28 were selected for the validation of the hydrodynamic jet break up model and the related heat transfer models. KROTOS-44, FARO L-33, and TROI-13 were selected for the simulation of the explosion fragmentation model and the relevant heat transfer models. The results of the simulation will form the basis for the reactor calculation.

## 2. The Evaluation of the Pre-mixing Model

The heat transfer correlations and the jet break up model are important analytical models. A comprehensive discussion on the results of the TEXAS-V simulation for the jet break up models and the relevant thermal-hydraulic model against the experimental data of FARO L-14 and L-28 is provided in Reference 3. Table 1, below, compares the major parameters of the two

**Table 1. Major Parameters of the FARO L-14 and L-28 Experiments**

	L-14	L-28
Corium Mass (kg)	125	175
Release diameter (m)	0.1	0.05
Pressure (MPa)	5.0	0.51
Sub-cooling (K)	0	0
Water Depth (m)	2.05	1.44
Gas volume (m <sup>3</sup> )	1.26	3.528
Water volume (m <sup>3</sup> )	0.798	0.564
Melt delivery (s)	1.0	5.21

experiments. In the case of L-28, the duration of the pour is much longer and it is at a low pressure.

The two break up models implemented in TEXAS-V were used in the analysis. Figure 1 shows that there was not much difference between the old break up model, which is based on Rayleigh Taylor instability, and the new break up model, which has more mechanistic break up mechanisms, including Rayleigh Taylor instability, boundary layer stripping, and Kelvin Helmholtz instability, in the simulation of FARO L-14. However, Fig. 2 shows that the two break up models do have quite different behavior in the case of FARO L-28.

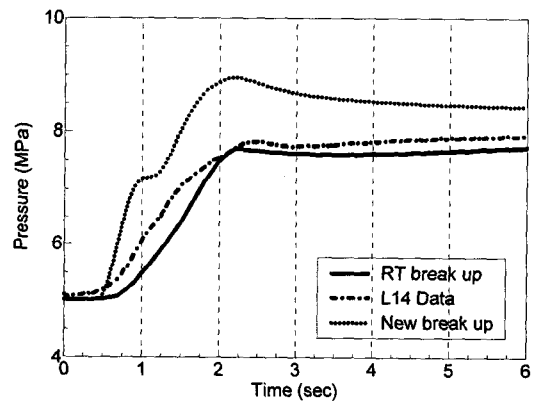


**Fig. 1. Comparison of Pressure for the L-14**

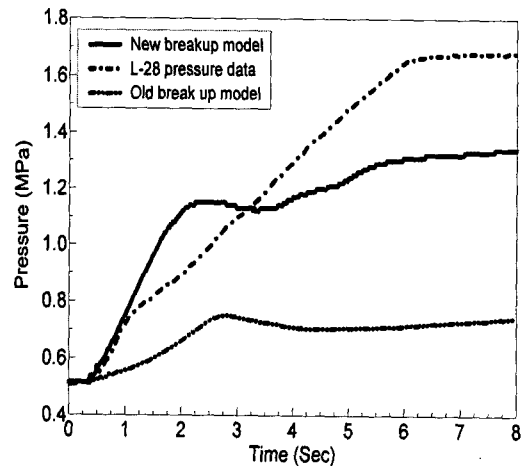


**Fig. 2. Comparison of Pressure for L-28**

It was shown that the computational model adequately predicted the jet break up model and the thermal hydraulic response during the premixing phase for a transient with a rather short pour at a high pressure. However, it was necessary to substantially increase the effectiveness of the Kelvin Helmholtz instability to match the L-28 pressure. This suggests that the break up model

needs to be improved further to adequately model the thermal-hydraulic response of the system and jet break up model during a rather long pour. Also, another fundamental difference between these two models is the system pressure. It is quite probable that the heat transfer correlations used in the computational model are tuned for high-pressure experiments.

**Table 2. Initial and Boundary Conditions**

	FARO L-33	KROTOS-44	TROI-13	TROI-34
Melt Composition	UO <sub>2</sub> /ZrO <sub>2</sub> , 80:20	Al <sub>2</sub> O <sub>3</sub>	UO <sub>2</sub> /ZrO <sub>2</sub> , 70:30	UO <sub>2</sub> /ZrO <sub>2</sub> , 70:30
Released Mass (kg)	100	1.45	7.7	10.5
Release Diameter (m)	0.05	0.03	0.02	0.02
Pressure (MPa)	0.41	0.1	0.1	0.1
Sub-cooling (K)	124	10	81	32
Melt Velocity (m/s)	1.3 - 3.0 m/s	~ 1m/s	~ 7 m/s	~ 7 m/s
Free Fall (m)	0.77	0.43	3.8	3.35
Water depth (m)	1.62	1.115	0.67	0.67
Gas volume (m <sup>3</sup> )	3.5	0.23	8.03	8.03
Pool Diameter (m)	0.71	0.2	0.6	0.6
External Trigger	Yes	Yes	No	Yes

**Table 3. Summary of the Analysis Results for the Explosion Phase Only**

	FARO L-33	KROTOS-44	TROI-13	TROI-34
Explosion only	Yes	Yes	Yes	Yes
Melt fraction /Total mass (kg)	0.026/25	0.026/1.5	0.000636/1.14	0.000636/1.14
Explosion Model Constants	R <sub>f</sub> =20μm, C <sub>fr</sub> =0.002 T <sub>fr</sub> = 1 ms	R <sub>f</sub> =20μm, C <sub>fr</sub> =0.002 T <sub>fr</sub> = 1 ms	R <sub>f</sub> =100μm, C <sub>fr</sub> =0.002 T <sub>fr</sub> = 1 ms	R <sub>f</sub> =100μm, C <sub>fr</sub> =0.002 T <sub>fr</sub> = 1 ms
Calculated Pressure (MPa)	100	75	3	25
Fuel Diameter (mm)	3.6	15	3	3
Pre-mixture Height (m)/Width(m)	1.7/0.3	0.75/0.2	0.7/0.2	0.7/0.2
Void fraction	0.05, uniform	0.09	0.04, uniform	0.04, uniform
Trigger	14MPa/14μs	14 MPa/ 1ms	Spontaneous	10MPa/0.2 ms

### 3. The Evaluation of the Explosion Model

KROTOS-44, FARO L-33, TROI-13, and TROI-34 were selected in the OECD/SERENA program to simulate the explosion fragmentation model and the relevant heat transfer models. Initial and boundary conditions for each experiment are provided in Table 2, and a brief summary of analysis results for the explosion phase only is provided in Table 3.

#### 3.1. Analytical Models

During the explosion, the TEXAS-V computer code uses a fragmentation model by Tang [5], which is presented as

$$M_f = C_{fr} m_p (P - P_{th}) / (\rho_c R_p)^{2/3} g(\tau) F(\alpha)$$

$P$  is the pressure of a computational cell,  $m_p$  is the mass of a master particle,  $\rho_c$  is the density of the coolant,  $C_{fr}$  is a parameter to match the experimental data, and  $P_{th}$  is the threshold pressure necessary to cause a film collapse. A study by Nelson [6] and Kim [7] indicate that the threshold pressure is between 0.2 - 0.4 MPa for tests at an atmospheric pressure. Each master fuel particle group has a corresponding group for its fragmented particles. We assume that all the fragmented fuel quenches to a coolant and gives its energy at once to the coolant in evaporating from a liquid to a vapor.  $R_p$  is the estimated size of the fragmented particles and  $\tau$  is the fuel fragmentation time interval; the factor  $g(\tau)$  decreases from 1 to zero as this characteristic time is exceeded. A compensating factor for the coolant void fraction  $F(\alpha)$  is introduced because the film collapse and coolant jet impingement gradually become less likely to occur as the void fraction increases. The factor decreases from 1 to 0 when the void fraction is above 0.3.

There was a sensitivity study for the effect of these parameters on the dynamic pressure. Tang [5] used  $C_{fr}$  at 0.001 and 0.002 for KROTOS-21 and KROTOS-26, respectively, and used ( between 0.2 to 4 ms. His study indicated that the pressure peak increases and the explosion wave propagates faster as the proportional constant  $C_{fr}$  increases. Nelson's experiment [8] indicated that as the ambient pressure increases, the characteristic time for the fragmentation decreases. However, as there is no data, the parameter is adjusted to match the KROTOS-21 (2 ms) and -26 (0.5 ms) data. Tang [5] also did a parametric study on the characteristic time (0.0012 and 0.012) and void fraction (0.27 - 0.35) for KROTOS-44 while keeping  $C_{fr}$  as 0.002. Based on these previous studies, here the standard values of  $C_{fr}=0.002$  and  $\tau = 1$  ms were chosen for the simulation of KROTOS-44.

#### 3.2. Analysis of the KROTOS-44 Test

The KROTOS-44 test belongs to a series of tests dedicated to the identification of explosion behavior using Alumina melt. It is one of the best experiments for the validation of the explosion model, as it is a kind of analytical experiment where the test section has a one-dimensional geometry and it has a strong constraint for the explosion to maximize the energy of the explosion. The configuration of the experiment is shown in Fig.3.

The initial condition for the pre-mixture was determined from the experimental data and was prescribed from the OECD/SERENA project. Just before the explosion, a pre-mixture is determined from the experimental data and is prescribed as the initial condition for the explosion calculation. It consists of volume fractions for each phase and component, mean particle diameter, liquid temperature, gas temperature, and melt

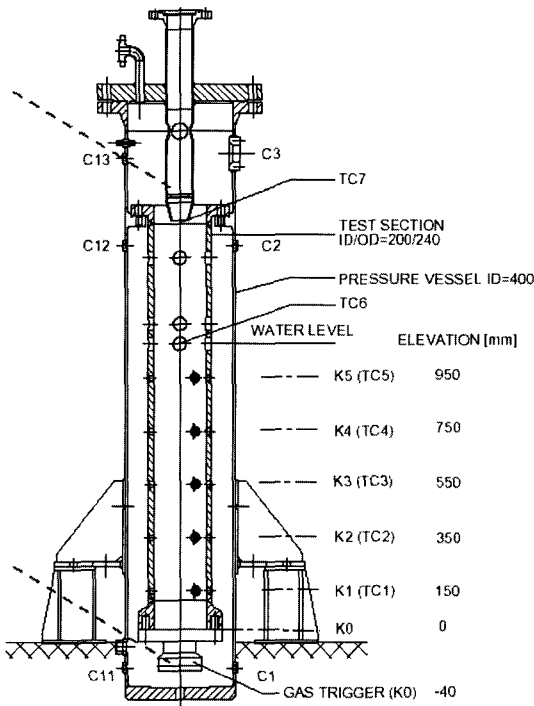


Fig. 3. The Geometry of the KROTOS Experiment

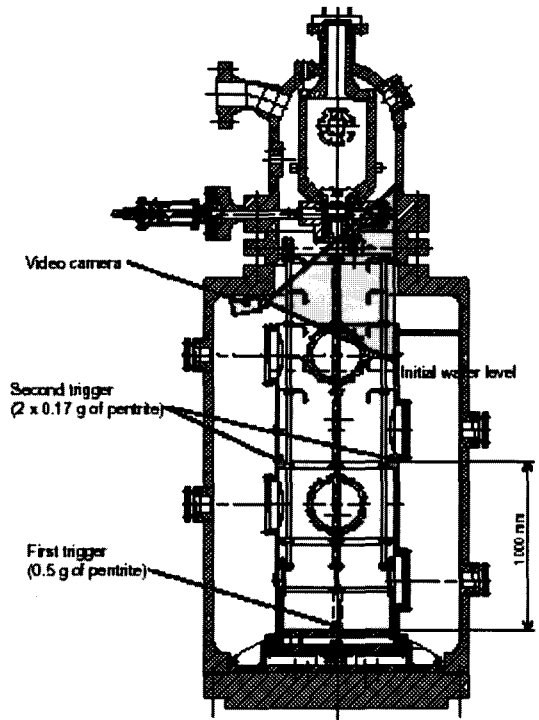


Fig. 4. Configuration of the FARO L-33 Test

temperature. Below the pre-mixture there is a water slug region. Above the pre-mixture there is a region consisting of a two-phase plug and cover gas. The explosion is triggered by an injection of high-pressure gas at the bottom. As the pre-mixture just before the explosion is well defined, this is a good analytical experiment for testing the explosion model in the computational model.

**3.2.1. The Input Model for TEXAS-V**

Though the TEXAS-V allows only one-dimensional nodes, it is suitable for the simulation of KROTOS-44 as the geometry and associated phenomena are nearly one-dimensional. The input model for KROTOS-44 has 30 nodes for simulation of the facility: 24 nodes are for the test vessel and the 6 nodes on the top are to simulate the cover gas region. The initial void fraction and

melt fraction in each region are initialized to match the prescribed conditions. To have a uniform melt fraction of 0.026 in the pre-mixture, particles are distributed in 10 cells with 31 particles per cell with  $d_p=15$  mm. The total weight of the fuel is 1.48 kg. The trigger cell is added at the bottom, which is filled with saturated steam at 14.8 MPa. The fluid temperature and cover gas pressure are specified per a given condition.

**3.2.2. Analysis Results**

After a very short initialization period, the trigger cell is activated to start the explosion calculation, the duration of which is 6 ms. The plot for the pressures measured at each pressure transducer for KROTOS-44 is shown in Fig.5. The calculated pressure is shown in Fig. 6.

The impulse on the vessel wall can be calculated

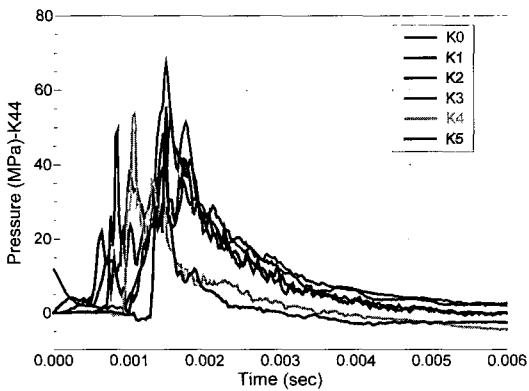


Fig. 5. Dynamic Pressure -(Measured)

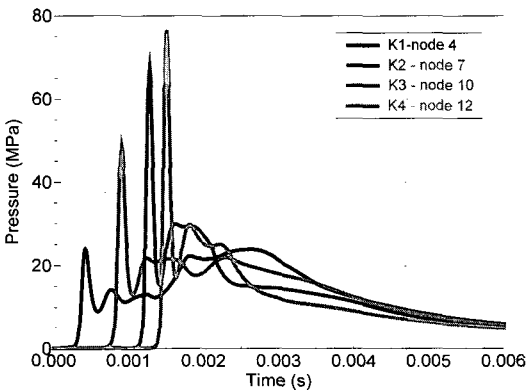


Fig. 6. Dynamic Pressure (Calculated)

from the time integral of the dynamic pressure on the wall in Figure 5. The value up to the maximum has a physical meaning. The shape and magnitude of the measured impulse and calculated impulse are nearly the same. Both curves reached 90 KN.s in 4 ms, which suggests that the explosion model in TEXAS-V has good predictability for an analytical experiment like KROTOS-44.

### 3.3. Analysis of FARO L-33

In this test, 100 kg of corium melt (80% wt  $UO_2$ , 20%wt  $ZrO_2$ ) at 3073 K was poured into a test section that contained 531 kg of water and had a depth, temperature, and pressure of 1.62 m, 294 K, and 0.41 MPa, respectively. Major parameters of the FARO L-33 test are listed in

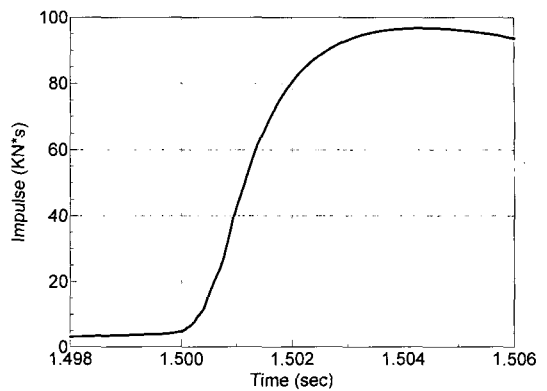


Fig. 7. Impulse on the Wall (Measured)

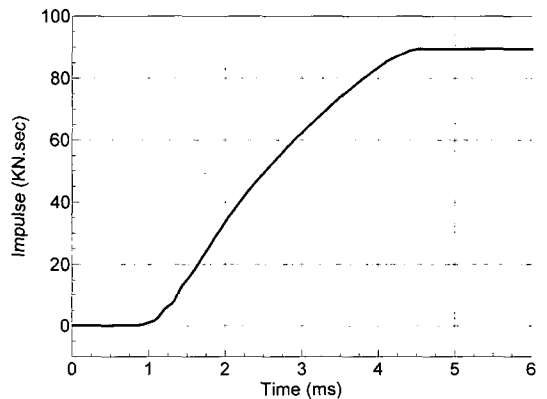


Fig. 8. Impulse on the Wall (Calculated)

Table 3, and the test configuration is shown in Fig. 4. The test section is contained in a FAT vessel, and an external trigger was applied at 1.12 s, which resulted in an energetic steam explosion. The maximum pressure measured on the wall of the test section was 10.5 MPa.

There are two ways to calculate the steam explosion load for this test. The first is to simulate the whole phase of the experiment, including both the pre-mixing phase and the explosion phase. An alternative approach is starting the calculation from a given pre-mixture condition. Here, the second approach is chosen to test the TEXAS-V explosion model separately. The pre-mixture condition that was given from the OECD/SERENA project is

briefly summarized in Table 3.

### 3.3.1. The Input Model for TEXAS-V

The input model for FARO L-33 has 44 nodes for the simulation of the facility. It has 34 nodes for the test vessel, which is 2.3 m in height, and has 10 nodes, each sized 0.1 m, on the top to simulate the cover gas region. The area of the nodes for the test vessel is 0.344 m<sup>2</sup>

There is certainly a multi-dimensional effect in the FARO L-33 tests, because the pre-mixture, with a height of 1.7 m and a diameter of 30 cm, is formed only near the center region of the test section. The initial void fraction of the test vessel was taken as 0.05, assuming a uniform distribution. However, as the TEXAS-V allows for only one-dimensional nodes, a uniform distribution of the fuel and void is assumed. This deficiency can be augmented by a parametric study on the size of the mixture zone.

A uniform melt fraction of 0.026 in the pre-mixture was simulated by distributing particles (size  $d_p=3.6$  mm) in the cell. The total weight of the fuel was 25 kg. A uniform void fraction of 0.05 was assumed in the pre-mixture. The trigger cell was added at the bottom, which was filled with saturated steam at 14 MPa.

### 3.3.2. Analysis Results

After a very short initialization period, the trigger cell was activated to start the explosion calculation. The duration of the explosion calculation was 6 ms. Plots for the pressures measured and calculated at each pressure transducer for FARO L-33 are shown in Fig. 9 and Fig. 10.

In this calculation, the key parameters are chosen as the same as those of the KROTOS-44 simulation. As can be seen from the plots, the

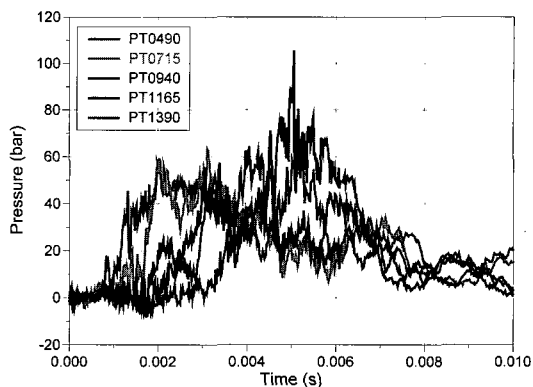


Fig. 9. Dynamic Pressure (Measured)

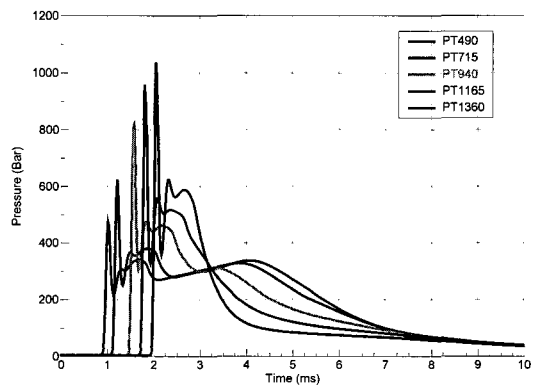


Fig. 10. Dynamic Pressure (Calculated)

calculated pressure is ten times greater than the measured pressure. This indicates that a steam explosion model fitted for the alumina/water system could give the bounding results for the corium/water system even though it is far from the best estimation. The other computer code also has same pattern in the default code settings [10]. In order to match the data, key effects such as the heat transfer and fragmentation parameters had to be more or less arbitrarily reduced. The fundamental difference is the material. Possible physical explanations are freezing of the melt during pre-mixing and hydrogen production during pre-mixing, which was observed in the FARO tests. However, as there is certainly an indication

that the corium is barely explosive, it is possible that there could be other effects not listed above. Further investigations are necessary to draw further conclusions.

### 3.4. Analysis of TROI-13 and TROI-34

Korea Atomic Energy Research Institute (KAERI) launched a research initiative on steam explosion named "Test for Real Corium Interaction with Water (TROI)" in 1997. After preliminary tests using  $ZrO_2$ , experiments using a mixture of  $ZrO_2$  and  $UO_2$  [11] were performed. About 4 ~ 9 kg of corium melt (80% wt  $UO_2$ , 20%wt  $ZrO_2$ ) jet was delivered into a sub-cooled water pool at an atmospheric pressure. Spontaneous steam

explosions occurred repeatedly. It was reported that the TROI-13 experiments resulted in a dynamic pressure of 7 MPa. It was observed that reactor material resulted in a spontaneous explosion, which is very important since previous experiments did not indicate this. The configuration of the recent TROI experiment is shown in Fig. 11. Fig. 12 is a typical snapshot of fuel coolant interaction in the TROI, which was measured by a high-speed video.

It was decided at the OECD/SERENA meeting to perform a blind test for the code simulation in the TROI in addition to in TROI-13. The test was performed at almost the same initial and boundary conditions as that for TROI-13, except for the use of an external trigger. Table 2 summarizes the major parameters of those two experiments. In the calculation, the major parameters are taken as the same as those of the KROTOS-44.

The dynamic pressure sensors, IVDP101, IVDP102, and IVDP103, were flush-mounted on the wall of the test section for TROI-13. In TROI-34, hanging dynamic pressure transducers, UWDP101 and UWDP102, were additionally

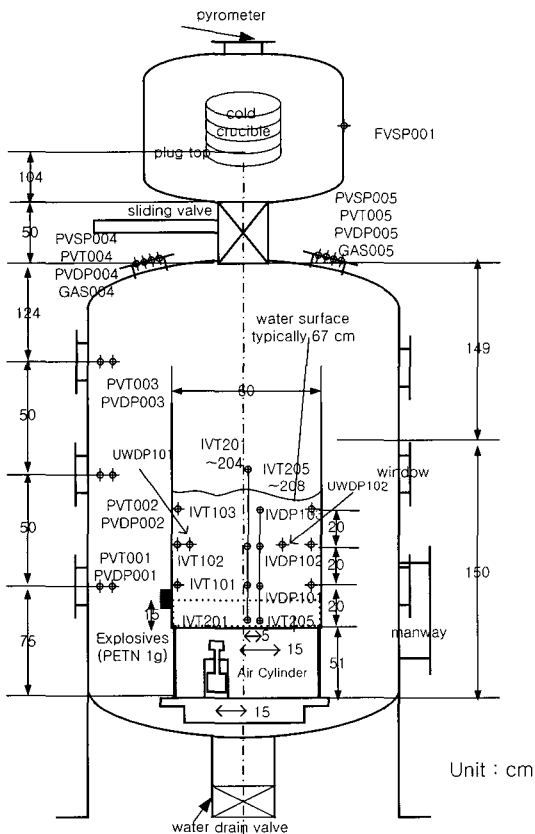


Fig. 11. Configuration of the TROI-34 Test

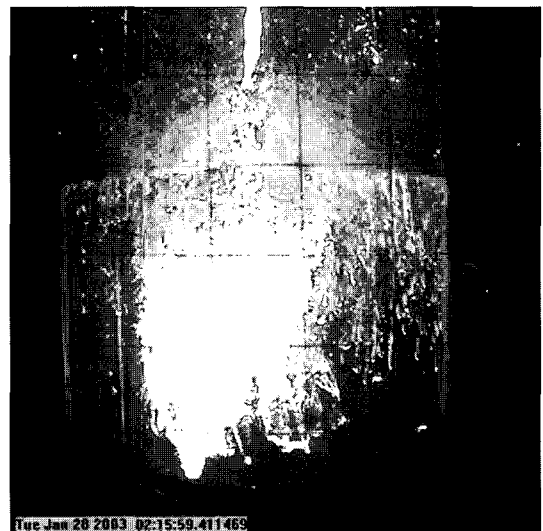


Fig. 12. Visualization of Fuel Coolant Interaction



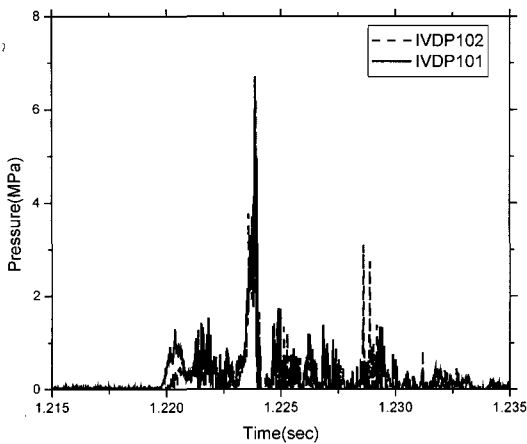


Fig. 13. Dynamic Pressure for TROI-13

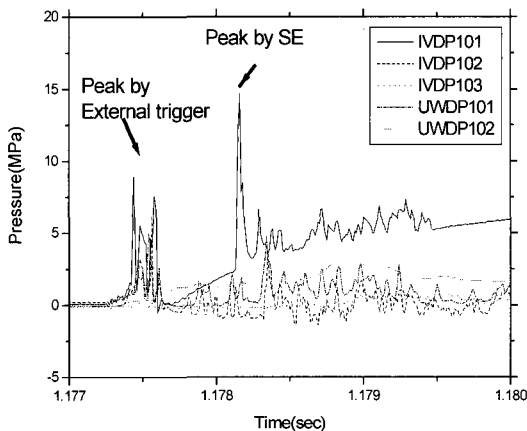


Fig. 14. Dynamic Pressure for TROI-34

installed near the wall in the water pool. In the TROI-34 test, there were two peaks in the dynamic pressures. The initial peak was due to the dynamic pressure caused by the external trigger, and the second peak was due to a real steam explosion. It is to be noted, however, that the dynamic pressure signal IVDP101 was affected by the thermal transient. Furthermore, the baseline signal was also affected by the thermal effect due to high temperature melt contact. However, we believe that the dynamic peak was not affected, as the duration was very short.

### 3.4.1. The Input Model for TROI

The input model for TROI-13 and 34 has 45 nodes for the simulation of the facility. It has 25 nodes for the test vessel, which is 1.5 m in height, and has 20 nodes, each sized 0.19 m, on the top to simulate the cover gas region. The area of the nodes for the test vessel is 0.283 m<sup>2</sup>.

There is a definite multi-dimensional effect in the TROI-13 tests because the pre-mixture is concentrated near the center region of the test section, as shown in Fig. 12. However, as the TEXAS-V allows only one-dimensional nodes, a uniform distribution of the fuel and the void is assumed. This deficiency can be augmented by a parametric study.

The initial void fraction of the test vessel was taken as 0.04, assuming a uniform distribution. A uniform melt fraction of 0.000636 in the pre-mixture was simulated by particles at a size of  $d_p=3.2$  mm that were distributed in the cell. The total weight of the fuel was 1.14 kg. The trigger cell was added at the bottom. The basic input data was the same for TROI-13 and TROI-34, except that the trigger was different. For TROI-13, a spontaneous trigger was modeled by activation of a steam explosion at every computational cell. In the TROI-34 analysis, a trigger cell filled with saturated steam at 10 MPa was added at the bottom.

### 3.4.2. Analyses Results for TROI-13 and TROI-34

The parameters for the explosion model were the same as those used in the simulation of the KROTOS-44. Figs. 15 and 16 show the calculated pressure.

It is shown that the calculated pressures are in the same order as the pressures of the experiments. The case with an external trigger showed a nice

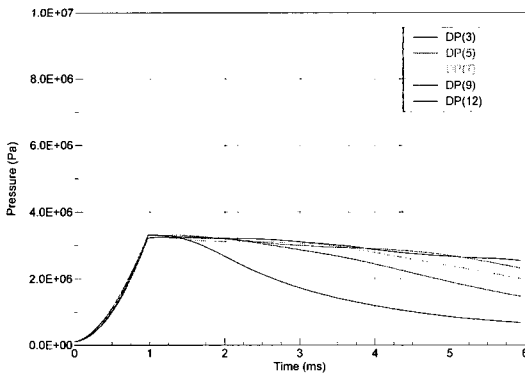


Fig. 15. Dynamic Pressure for TROI-13

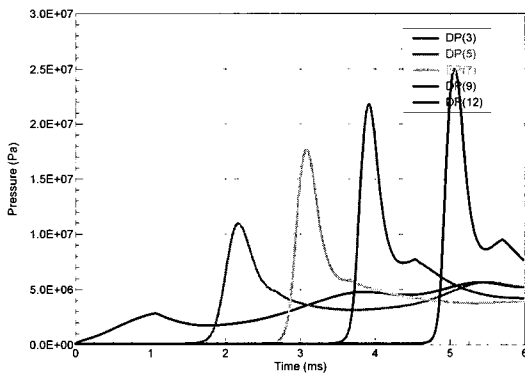


Fig. 16. Dynamic Pressure for TROI-34

propagation of the explosion wave. However, this behavior was not observed in the TROI-34 experiments. In the case of a spontaneous steam explosion, the calculated behavior was quite similar to the experimental observations. It was interesting that the calculated pressure was lower than the experimental measurement.

These findings are quite inconsistent with those of FARO L-33. The main difference is the fuel fraction. The fuel fraction is in a smaller magnitude of order than that of FARO L-33, and this low fuel fraction could have resulted in the low dynamic pressure. It can be claimed that the TEXAS-V computer code predicts the dynamic pressure in the same order of magnitude for experiments at a very low fuel fraction.

Another possible explanation involves noting that the void fraction in the interaction region is close to 40% when we convert the level swell measured in a normal high-speed video, the typical shape of which is shown in Fig. 12. Since the explosion could not propagate in a highly voided region, the explosion must have occurred near the outer boundary of the interaction zone, where the void fraction is low. Then, the amount of fuel participating in the interaction could be very small. However, this type of multi-dimensional phenomena cannot be easily predicted with the existing steam explosion computer codes.

#### 4. Discussions and Summary

The analyses in this paper have been focused on evaluating the pre-mixing model and the explosion model separately. So, the next step should be an evaluation of the adequacy of computer codes in simulating the entire phase of the steam explosion. The present analysis provides a firm cornerstone for the integral calculation in the sense that the major parameters for the pre-mixing model and the explosion model have been tested and selected from analyses of carefully selected experiments.

Uncertainties still exist, however, in areas such as the multi-dimensional effect, material effect, freezing phenomena, and hydrogen generation. However, the present analysis demonstrates that the TEXAS-V could be a promising tool in predicting the steam explosion load on a reactor scale, as the analysis results with the default parameter setting predicted the experimental results reasonably well. Also, as a fast running computer code, the TEXAS-V allows the user to perform a sensitivity study to evaluate the impact of various uncertainties, which are not clearly understood yet, to provide a conservative envelope

for the steam explosion load on a reactor condition. Reducing the possibility of steam explosions is essential for the design of preventive measures.

### Acknowledgement

The present research is supported by Korea Ministry of Science and Technology (MOST), under the national nuclear mid- and long-term research and development program.

### References

1. Carbiener, W. A. et al., Appendix VIII in Reactor Safety Study, WASH-1400 (NUREG-75/014), (1975).
2. Magallon et. al, Proposal for a OECD research programme on fuel-coolant interaction-Steam Explosion Resolution for Nuclear Applications (SERENA), (2001).
3. J. H. Song, I. K. Park, S. Nilsuwankosit, Evaluation of the TEXAS-V break up models against experimental data, 11<sup>th</sup> conference on nuclear engineering, Tokyo, Japan, ICONE11-36155, (2003).
4. I. K. Park, D. H. Kim, and J. H. Song, Steam explosion module development for the MELCOR code using TEXAS-V, Journal of Korean Nuclear Society, Vol. 35, Number 4, pp.286-298, (2003).
5. J. Tang, Modeling of the complete process of one-dimensional vapor explosions, Ph. D. Thesis, University of Wisconsin, (1993).
6. Nelson, L. S. and Duda, P. M. Steam explosion experiments with single drops of iron oxide melted with a CO<sub>2</sub> laser: Part II. Parametric studies. SAND82-1105, SNL, (1985).
7. Kim, H. Single droplet vapor explosion experiments, Ph. D. Thesis, University of Wisconsin, (1987).
8. B. Kim, M. Corradini, Modeling of small-scale single droplet fuel/coolant interactions, Nuc. Sci. Eng, 98, 16-28, (1988).
9. Annunziato, A., Addabbo, A., Leva, G., OECD/CSNI international standard problem No. 39 on FARO test L-14, Technical Note No. I.96.64, Joint Research Center, (1996).
10. D. Magallon, Summary conclusions and actions from 3<sup>rd</sup> SERENA meeting, Aix-en-Provence, May 15-18, France, (2004).
11. J. H. Song et al., Fuel Coolant Interaction Experiments in TROI Using a UO<sub>2</sub>/ZrO<sub>2</sub> Mixture, Nuclear Engineering and Design, Vol.222, 1-15, (2003).
12. J. H. Kim et al., Phenomenological Studies of Steam Explosions Triggered by an External Trigger in the TROI Experiment, Proceedings of Korean Nuclear Society Spring Meeting, May, (2004).